

# Asymptotic fields in the finite element analysis of electrically permeable interface cracks in piezoelectric bimetaterials

V. Govorukha, M. Kamlah

92

**Summary** The interface crack problem for a piezoelectric bimaterial based on permeable conditions is studied numerically. To find the singular electromechanical field at the crack tip, an asymptotic solution is derived in connection with the conventional finite element method. For mechanical and electrical loads, the complex stress intensity factor for an interface crack is obtained. The influence of the applied loads on the electromechanical fields near the crack tip is also studied. For a particular case of a short crack with respect to the bimaterial size, the numerical results are compared with the exact analytical solutions, obtained for a piezoelectric bimaterial plane with an interface crack.

**Keywords** Interface crack, Piezoelectric material, Finite element analysis, Stress intensity factor

## 1

### Introduction

Due to the intrinsic coupling effects that take place between electric and mechanical fields, piezoelectric materials have been extensively used as sensors, transducers and actuators. They play a key role in the development of electromechanical systems in electronics, micro-system technology, mechatronics or adaptive structures. However, their applications are restricted by the brittleness of the commonly used piezoceramic materials. When subjected to loading, these materials may fail prematurely due to the propagation flaws or defects induced during the manufacturing process and by the in-service electromechanical loading. Therefore, it is important to understand and be able to analyze the fracture characteristics of piezoelectric materials, so that reliable service life predictions of the pertinent devices can be conducted. In this light, a large amount of analytical works have been devoted to the fracture mechanics of piezoelectric materials, [1–5].

Modeling and simulation of the electromechanical field in the vicinity of the crack tip allows for a better insight into the failure modes of the piezoelectric materials. The use of the finite element method (FEM) in fracture mechanics has become increasingly popular, and the degree of its accuracy depends on the method of representing or accounting for the singularity associated with the crack tip.

For *homogeneous* piezoelectric materials, various types of FE approaches have been developed, using conventional or singular crack finite elements. Comprehensive work on the use of FE techniques in fracture mechanics of these materials has been presented in [6–9].

---

Received 6 February 2004; accepted for publication 7 June 2004

V. Govorukha (✉)  
Dept. of Computational Mathematics,  
Dnepropetrovsk National University,  
49050 Dnepropetrovsk, Ukraine  
Corresponding author.  
e-mail: govor@amsu.dnp.ukrpack.net

M. Kamlah  
Forschungszentrum Karlsruhe,  
Institut for Materials Research II, Postfach 3640,  
76021 Karlsruhe, Germany

One author (V.G.) gratefully acknowledges the support provided by the Alexander von Humboldt Foundation of Germany.

For piezoelectric *bimaterials*, the situation is more complicated since the field equations are complex and the calculation of fracture parameters is far from obvious. It is well known that the rate of convergence of a conventional FE solution in the presence of a crack tip singularity is slow and can not be improved by employing high-order interpolations. Therefore, for correct numerical solutions the exclusive use of the FEM is not always sufficient. A special element incorporating an analytical solution for piezoelectric bimaterial was developed for the first time, in [10] by the use of asymptotic eigenfunction expansions in connection with the conventional FEM.

The present work employs the combination of the analytical and FE solution to determine the singular field of an interfacial crack between two piezoelectric materials subjected to external electromechanical load. In addition, a straightforward method is presented for evaluating the complex stress intensity factor (SIF) for interfacial cracks in piezoelectric bimaterials. The presentation of the numerical techniques is restricted here to the permeable case, but extensions to other crack face boundary conditions are possible.

## 2

### Basic equations

The foundations of fracture mechanics for linear piezoelectric materials can be found in [11]. The constitutive equations can be written as

$$\sigma_{ij} = c_{ijkl}\gamma_{kl} - e_{kij}E_k, \quad (1)$$

$$D_i = e_{ikl}\gamma_{kl} + \varepsilon_{ik}E_k, \quad (2)$$

where,  $\sigma_{ij}, \gamma_{ij}$  are the stress and strain tensors, respectively;  $D_i, E_i$  are the electric displacement and electric field;  $c_{ijkl}, e_{ijkl}, \varepsilon_{ij}$ , are the elastic, piezoelectric and dielectric constants.

It is assumed that inside the piezoelectric block there are no body forces and body charges. Consequently, the mechanical and electrical equilibrium equations take the form

$$\sigma_{ij,i} = 0, \quad (3)$$

$$D_{i,i} = 0, \quad (4)$$

where a comma indicates partial differentiation with regard to the respective coordinate.

Strain  $\gamma_{ij}$  and electric field  $E_i$  can be expressed as

$$\gamma_{ij} = \frac{1}{2}(u_{i,j} + u_{j,i}), \quad (5)$$

$$E_i = -\varphi_{,i}, \quad (6)$$

where  $u_i$  are the displacements and  $\varphi$  is the electric potential.

The conditions at the outer boundary of the block are the following

$$\sigma_{ij}n_j = T_i, \quad (7)$$

$$D_jn_j = -\omega_s, \quad (8)$$

where  $n_i$  is the outer unit normal vector of the surface;  $T_i$  is the applied surface traction and  $\omega_s$  is the applied surface charge. Together they define the external electromechanical load.

For the electrically permeable crack face, the electric potential and the normal electric displacement should be continuous across the crack slit

$$D_n^+ = D_n^-, \quad \varphi^+ = \varphi^-. \quad (9)$$

## 3

### Asymptotic field equations near the crack tip

Consider a piezoelectric solid in a cartesian coordinate system  $x_j (j = 1, 2, 3)$ . The attention is focused in the following on piezoelectric materials poled in the direction  $x_3$  which have an

essential practical significance as so-called poled ceramics. In this case, for loads which are independent of the coordinate  $x_2$ , we can look for fields in the  $(x_2, x_3)$  -plane, where the displacement  $u_2$  decouples from the components  $(u_1, u_3, \varphi)$ . As the  $u_2$ -determination is simple, our attention will be focused on the plane problem for the components  $(u_1, u_3, \varphi)$ . In this case, according to the Stroh formalism, the general solution for the two-dimensional problem can be expressed as [4],

$$\mathbf{U} = \mathbf{A}\mathbf{f}(\mathbf{z}) + \overline{\mathbf{A}}\overline{\mathbf{f}}(\overline{\mathbf{z}}), \quad (10)$$

$$\mathbf{t} = \mathbf{B}\mathbf{f}'(\mathbf{z}) + \overline{\mathbf{B}}\overline{\mathbf{f}}'(\overline{\mathbf{z}}), \quad (11)$$

with

$$\mathbf{U} = [u_1, u_3, \varphi]^T, \quad \mathbf{t} = [\sigma_{13}, \sigma_{33}, D_3]^T, \quad \mathbf{f}(\mathbf{z}) = [f_1(z_1), f_2(z_2), f_3(z_3)]^T, \quad z_k = x_1 + p_k x_3, (k=1, 2, 3).$$

In the above equations, the superscript  $T$  represents the transpose; the overbar stands for the conjugate of a complex value;  $\mathbf{A}$  and  $\mathbf{B}$  are  $(3 \times 3)$ -matrices which can be determined via the material constants;  $f_k(z_k)$  are complex potentials to be found;  $p_k$  are the distinct complex eigenvalues with positive imaginary parts.

Since we are only interested in the leading asymptotic field near the crack tip, we treat the crack as a semi-infinite crack with  $x_1$  in the crack plane and  $x_3$  normal to the crack plane as shown in Fig. 1. Anticipating a power type of singularity, let us assume that the near-tip fields are of the following forms, [12]:

$$U_i(x_1, x_3) = \sum_{k=1}^3 [A_{ik} q_k z_k^\lambda + \bar{A}_{ik} v_k \bar{z}_k^\lambda], \quad (12)$$

$$t_i(x_1, x_3) = \sum_{k=1}^3 \lambda [B_{ik} q_k z_k^{\lambda-1} + \bar{B}_{ik} v_k \bar{z}_k^{\lambda-1}], \quad (13)$$

in which  $q_k$  and  $v_k$  are constants which must be determined from imposed boundary conditions. We look for admissible values of  $\lambda$  as well subject to the restriction  $0 < \text{Re}(\lambda) < 1$ .

The problem becomes more tractable if we introduce a polar coordinate system  $(r, \theta)$  as illustrated in Fig. 1. In this system defined by

$$x_1 = r \cos \theta, \quad x_3 = r \sin \theta, \quad (14)$$

the complex variable  $z_k$  becomes

$$z_k = r(\cos \theta + p_k \sin \theta). \quad (15)$$

Noticing that [13],

$$Z_k = \begin{cases} r, & \text{when } \theta = 0, \\ re^{\pm i\pi}, & \text{when } \theta = \pm\pi, \end{cases}$$

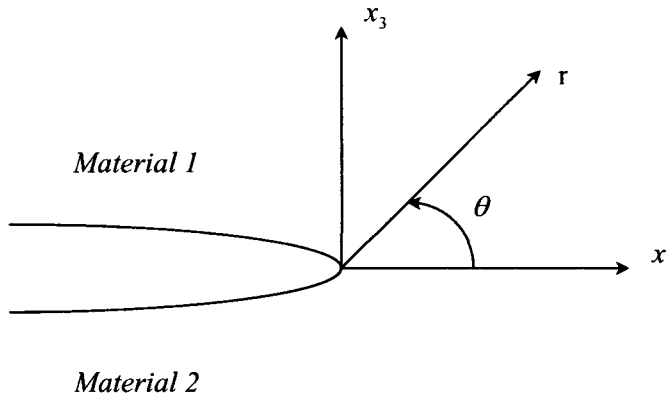


Fig. 1. Coordinate definitions for an interface crack

equations (12) and (13) yield

$$\mathbf{U}(r, 0) = r^\lambda [\mathbf{A}\mathbf{q} + \bar{\mathbf{A}}\mathbf{V}], \quad (16)$$

$$\mathbf{t}(r, 0) = r^{\lambda-1} \lambda [\mathbf{B}\mathbf{q} + \bar{\mathbf{B}}\mathbf{v}], \quad (17)$$

$$\mathbf{U}(r, \pm\pi) = r^\lambda \left[ e^{\pm i\pi\lambda} \mathbf{A}\mathbf{q} + e^{\pm i\pi\lambda} \bar{\mathbf{A}}\mathbf{v} \right], \quad (18)$$

$$\mathbf{t}(r, \pm\pi) = -r^{\lambda-1} \lambda \left[ e^{\pm i\pi\lambda} \mathbf{B}\mathbf{q} + e^{\pm i\pi\lambda} \bar{\mathbf{B}}\mathbf{v} \right], \quad (19)$$

where  $\mathbf{q}$  and  $\mathbf{v}$  are  $(1 \times 3)$  matrices with elements  $q_k$  and  $v_k$  ( $k=1, 2, 3$ ), respectively.

The unknown  $\mathbf{q}$ ,  $\mathbf{v}$  and  $\lambda$  will be determined by solving the system of equations subjected to boundary and interface conditions. The interface conditions can be stated as

$$\mathbf{U}^{(1)}(r, 0) = \mathbf{U}^{(2)}(r, 0), \quad \mathbf{t}^{(1)}(r, 0) = \mathbf{t}^{(2)}(r, 0). \quad (20)$$

Electrically permeable conditions along the crack surfaces require

$$\mathbf{t}^{(1)}(r, \pi) = \mathbf{t}^{(2)}(r, -\pi), \quad \sigma_{13}^{(1)}(r, \pi) = 0, \quad \sigma_{33}^{(1)}(r, \pi) = 0, \quad \varphi^{(1)}(r, \pi) = \varphi^{(2)}(r, -\pi), \quad (21)$$

where superscripts 1 and 2 denote materials 1 and 2, respectively.

By introducing the matrix  $\mathbf{Y} = i\mathbf{A}(\mathbf{B})^{-1}$  and defining

$$\mathbf{Q} = \mathbf{B}\mathbf{q}, \quad \mathbf{V} = \bar{\mathbf{B}}\mathbf{v}, \quad (22)$$

Eqs. (20) and (21a,b) can be rewritten as

$$\mathbf{Y}^{(1)}\mathbf{Q}^{(1)} - \bar{\mathbf{Y}}^{(1)}\mathbf{V}^{(1)} = \mathbf{Y}^{(2)}\mathbf{Q}^{(2)} - \bar{\mathbf{Y}}^{(2)}\mathbf{V}^{(2)}, \quad (23)$$

$$\mathbf{Q}^{(1)} + \mathbf{V}^{(1)} = \mathbf{Q}^{(2)} + \mathbf{V}^{(2)}, \quad (24)$$

$$e^{i\pi\lambda}\mathbf{Q}^{(1)} + e^{-i\pi\lambda}\mathbf{V}^{(1)} = e^{-i\pi\lambda}\mathbf{Q}^{(2)} + e^{i\pi\lambda}\mathbf{V}^{(2)}, \quad (25)$$

$$e^{i\pi\lambda}\mathbf{M}_1\mathbf{Q}^{(1)} + e^{-i\pi\lambda}\mathbf{N}_1\mathbf{V}^{(1)} = e^{-i\pi\lambda}\mathbf{M}_2\mathbf{Q}^{(2)} + e^{i\pi\lambda}\mathbf{N}_2\mathbf{V}^{(2)}, \quad (26)$$

where

$$\mathbf{M}_1 = \begin{bmatrix} 1 & 0 & 0 \\ 0 & 1 & 1 \\ Y_{31}^{(1)} & Y_{32}^{(1)} & Y_{33}^{(1)} \end{bmatrix}, \quad \mathbf{N}_1 = \begin{bmatrix} 1 & 0 & 0 \\ 0 & 1 & 1 \\ -\bar{Y}_{31}^{(1)} & -\bar{Y}_{32}^{(1)} & -\bar{Y}_{33}^{(1)} \end{bmatrix},$$

$$\mathbf{M}_2 = \begin{bmatrix} 0 & 0 & 0 \\ 0 & 0 & 0 \\ Y_{31}^{(2)} & Y_{32}^{(2)} & Y_{33}^{(2)} \end{bmatrix}, \quad \mathbf{N}_2 = \begin{bmatrix} 0 & 0 & 0 \\ 0 & 0 & 0 \\ -\bar{Y}_{31}^{(2)} & -\bar{Y}_{32}^{(2)} & -\bar{Y}_{33}^{(2)} \end{bmatrix}.$$

Eliminating  $\mathbf{V}^{(1)}$ ,  $\mathbf{Q}^{(2)}$ ,  $\mathbf{V}^{(2)}$  from the above four sets of equations leads to the following system:

$$[\mathbf{H} + e^{i2\pi\lambda}\bar{\mathbf{H}}\mathbf{W}]\mathbf{Q}^{(1)} = 0, \quad (27)$$

where

$$\mathbf{H} = \mathbf{Y}^{(1)} + \bar{\mathbf{Y}}^{(2)}, \quad \mathbf{W} = \begin{bmatrix} 1 & 0 & 0 \\ 0 & 1 & 0 \\ 0 & -2H_{32}/H_{33} & -1 \end{bmatrix},$$

To find nontrivial solutions, the determinant of the matrix of coefficients in Eq. (27) must vanish. The characteristic equation for the eigenvalue  $\lambda$  follows as

$$|\mathbf{H} + e^{i2\pi\lambda}\bar{\mathbf{H}}\mathbf{W}| = 0,$$

or

$$s(e^{i2\pi\lambda})^2 + pe^{i2\pi\lambda} + s = 0, \quad (28)$$

where

$$s = -H_{11}H_{22}H_{33} + 2H_{12}H_{13}H_{23} + H_{11}H_{23}^2 - H_{12}^2H_{33} - H_{13}^2H_{22},$$

$$p = 2[-H_{11}H_{22}H_{33} + H_{11}H_{23}^2 - 2H_{12}H_{13}H_{23} + 2H_{13}^2H_{23}^2/H_{33} - H_{13}^2H_{22} + H_{12}^2H_{33}].$$

Equation (28) has two complex solutions, which are conjugates of each other and are given by the formulas

$$\lambda = (0.5 + n) \pm i\varepsilon, \quad \varepsilon = \frac{1}{2\pi} \ln \left( \frac{p}{2s} - \sqrt{\left(\frac{p}{2s}\right)^2 - 1} \right), \quad n = 0, 1, 2, \dots \quad (29)$$

The eigenvectors  $\mathbf{q}$  and  $\mathbf{v}$  associated with an eigenvalue  $\lambda$  can be found from (22).

The smallest eigenvalue ( $n = 0$ ) in the region  $0 < \text{Re}(\lambda) < 1$  characterizes the order of the singularity at the crack tip. Hence, the electromechanical fields around the crack tip can be presented as follows:

$$U_i(r, \theta) = 2\text{Re}\{Cr^\lambda\Phi_i(\theta)\}, \quad (30)$$

$$t_i(r, \theta) = 2\text{Re}\{Cr^{\lambda-1}\Psi_i(\theta)\}, \quad (i = 1, 2, 3) \quad (31)$$

where

$$\Phi_i(\theta) = \sum_{k=1}^3 \left[ A_{ik}q_k(\cos\theta + p_k \sin\theta)^\lambda + \bar{A}_{ik}v_k(\cos\theta + \bar{p}_k \sin\theta)^\lambda \right],$$

$$\Psi_i(\theta) = \sum_{k=1}^3 \lambda \left[ B_{ik}q_k(\cos\theta + p_k \sin\theta)^{\lambda-1} + \bar{B}_{ik}v_k(\cos\theta + \bar{p}_k \sin\theta)^{\lambda-1} \right]$$

and  $C$  is an undetermined complex constant. This asymptotic solution dominating the behaviour in the neighbourhood of the crack tip will be combined with the FE solution of the full problem. As shown in the next section,  $C$  will be determined by matching the two solutions.

#### 4

##### Numerical results and discussion

In order to test the suggested FE techniques for crack analysis, the method is being applied to a crack at the interface between two different piezoelectric materials in the piezoelectric block, see Fig. 2. The length of the interface crack is 1/10 of the block size. The crack is oriented in the  $x_1$ -direction, perpendicular to the applied tension  $\sigma_{33}^{ext}$  and applied electric displacement  $D_3^{ext}$ . The piezoelectric block is polarized homogeneously in the  $x_3$ -direction. The geometry and the loading allow us to use some symmetries. For the calculation of the fields, a half-model is used, which contains the right-hand side of the block. The FE calculations are performed with a two-dimensional mesh which is refined at the crack tip Fig. 3. For the calculations, the FE program ABAQUS, [14], is used. The chosen element type is a regular eight-node biquadratic plane strain piezoelectric quadrilateral with reduced integration, [14]. The length of the smallest element at the crack tip was  $3 \times 10^{-8}$  of the crack length (no quarter-point technique has been used). The piezoelectric block sketched in Fig. 2 is loaded by a tensile stress of  $\sigma_{33}^{ext} = 10\text{MPa}$  and by an electric displacement of  $D_3^{ext} = 0.01\text{C/m}^2$ . The material parameters of PZT-4 and PZT-5H used for these calculations, are taken from [15] and [2], respectively. Under these loads, the FE calculations are performed for a permeable interface crack (boundary condition (9)). The accuracy of the present method is investigated by comparison of the obtained results

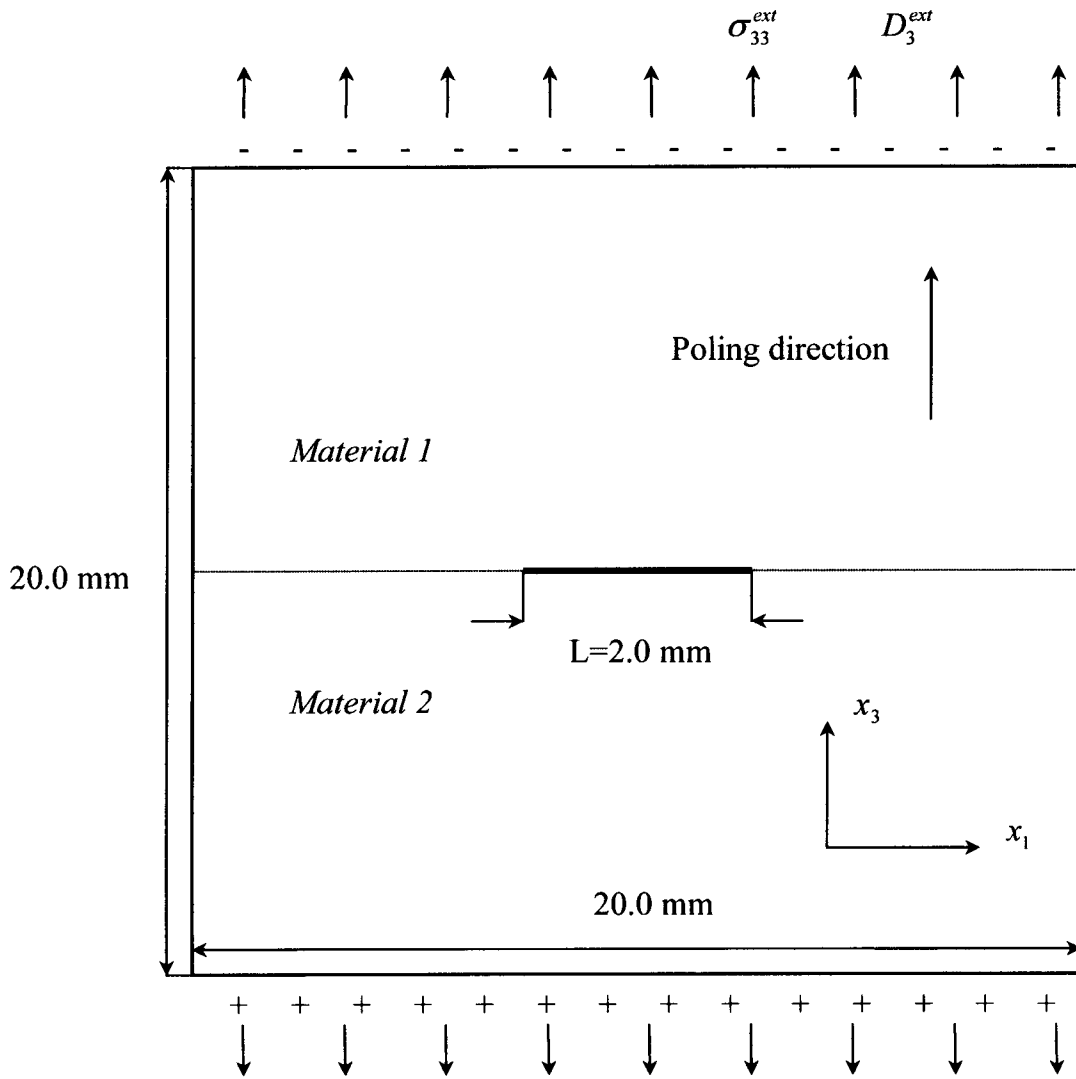


Fig. 2. Geometry and loading of the piezoelectric block ( $\sigma_{33}^{ext} = 10\text{MPa}$ ,  $D_3^{ext} = 0.01\text{C/m}^2$ )

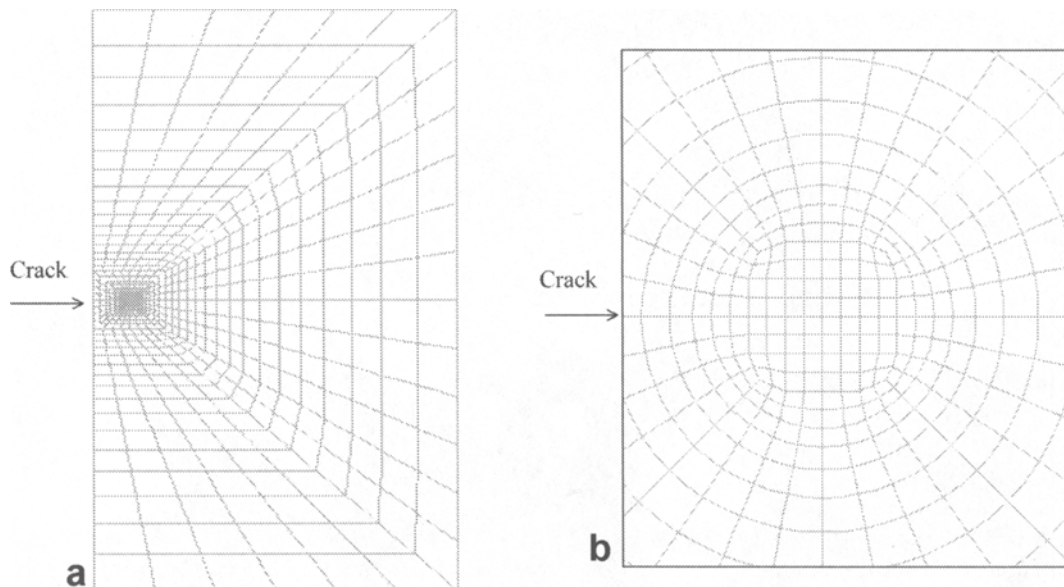


Fig. 3. The finite element mesh (a) for the piezoelectric bimaterial block with an interface crack; (b) local part of the mesh in the vicinity of the crack tip

to the exact analytical solution of the interface crack problem between two different piezo-electric semi-infinite planes given in [16].

The complex SIF introduced in [17] for the right hand side crack tip is

$$K_1 + iK_2 = \sqrt{2\pi r} r^{-i\epsilon} [\sigma_{33}(r, 0) + i\sigma_{13}(r, 0)] \quad (32)$$

According to this definition, one is able to express the complex Sif associated with smallest eigenvalue ( $\lambda = 0.5 + i\epsilon$ ) and eigenfunction  $\Psi_1(0), \Psi_2(0)$  as follows:

$$K_1 + iK_2 = \sqrt{2\pi C} [\Psi_2(0) + i\Psi_1(0)] \quad (33)$$

The asymptotic solution in the neighborhood of the interface crack tip, which has been derived in Sect. 3, must be adjusted to the FE solution obtained for the overall region of the problem in question. We perform this adjustment at the distance  $r = r_0$  from the crack tip. Since the unknown constant  $C$  is complex ( $C = \text{Re}C + i\text{Im}C$ ), it is necessary to formulate two adjustment conditions at  $r = r_0$  for the determination of the analytical parameters  $\text{Re}C$  and  $\text{Im}C$ . The numerical analysis shows that the best results correspond to the case when the adjustment conditions are taken at the bonded or cracked segments of the interface. Therefore in order to determine the constant  $C$ , conditions

$$\sigma_{33}^{(asym)}(r_0, 0) = \sigma_{33}^{(FEM)}(r_0, 0), \quad \sigma_{13}^{(asym)}(r_0, 0) = \sigma_{13}^{(FEM)}(r_0, 0) \quad (34)$$

can be used at the bonded segments of the interface. In this case, electric displacement  $D_3$  is proportional to  $\sigma_{33}$ . As an alternative, the conditions

$$[u_1(r_0)]^{(asym)} = [u_1(r_0)]^{(FEM)}, \quad [u_3(r_0)]^{(asym)} = [u_3(r_0)]^{(FEM)} \quad (35)$$

can be formulated at the cracked segment of the interface, where

$$[u_i(r)] = u_i^{(1)}(r, \pi) - u_i^{(2)}(r, -\pi) \quad (i = 1, 3)$$

designate the displacement jump.

The conditions (34) lead to the expressions

$$\begin{aligned} \text{Re}C &= \frac{\text{Im}[r_0^{\lambda-1}\Psi_2(0)]\sigma_{13}^{(FEM)}(r_0, 0) - \text{Im}[r_0^{\lambda-1}\Psi_1(0)]\sigma_{33}^{(FEM)}(r_0, 0)}{2(\text{Re}[r_0^{\lambda-1}\Psi_1(0)]\text{Im}[r_0^{\lambda-1}\Psi_2(0)] - \text{Im}[r_0^{\lambda-1}\Psi_1(0)]\text{Re}[r_0^{\lambda-1}\Psi_2(0)])}, \\ \text{Im}C &= \frac{\text{Re}[r_0^{\lambda-1}\Psi_2(0)]\sigma_{13}^{(FEM)}(r_0, 0) - \text{Re}[r_0^{\lambda-1}\Psi_1(0)]\sigma_{33}^{(FEM)}(r_0, 0)}{2(\text{Re}[r_0^{\lambda-1}\Psi_1(0)]\text{Im}[r_0^{\lambda-1}\Psi_2(0)] - \text{Im}[r_0^{\lambda-1}\Psi_1(0)]\text{Re}[r_0^{\lambda-1}\Psi_2(0)])}, \end{aligned} \quad (36)$$

for the unknown constant  $C$ , while the expressions

$$\begin{aligned} \text{Re}C &= \frac{\text{Im}[F_1(r_0)][u_3(r_0)]^{(FEM)} - \text{Im}[F_2(r_0)][u_1(r_0)]^{(FEM)}}{2(\text{Im}[F_1(r_0)]\text{Re}[F_2(r_0)] - \text{Re}[F_1(r_0)]\text{Im}[F_2(r_0)])}, \\ \text{Im}C &= \frac{\text{Re}[F_1(r_0)][u_3(r_0)]^{(FEM)} - \text{Re}[F_2(r_0)][u_1(r_0)]^{(FEM)}}{2(\text{Im}[F_1(r_0)]\text{Re}[F_2(r_0)] - \text{Re}[F_1(r_0)]\text{Im}[F_2(r_0)])}, \end{aligned} \quad (37)$$

with

$$F_1(r_0) = r_0^\lambda [\Phi_1^{(1)}(\pi) - \Phi_1^{(2)}(-\pi)], \quad F_2(r_0) = r_0^\lambda [\Phi_2^{(1)}(\pi) - \Phi_2^{(2)}(-\pi)],$$

follow from the conditions (35).

Table 1 shows the results for the SIF at purely mechanical loading ( $\sigma_{33}^{ext} = 10\text{MPa}$ ) with various values of  $r_0$  by means of the conditions (34) (columns 2,3) and the conditions (35) (columns 4, 5). The relative errors of these results with respect to the exact analytical solution

**Table 1.** Comparison of exact and numerical values of stress intensity factors for different adjustment conditions ( $\sigma_{33}^{ext} = 10\text{MPa}$ )

| $r_0/L$               | Adjustment conditions (34) |                           | Adjustment conditions (35) |                           |
|-----------------------|----------------------------|---------------------------|----------------------------|---------------------------|
|                       | $K_1(\text{MPa}\sqrt{m})$  | $K_2(\text{MPa}\sqrt{m})$ | $K_1(\text{MPa}\sqrt{m})$  | $K_2(\text{MPa}\sqrt{m})$ |
| $0.1 \times 10^{-6}$  | 0.512257 (8.01%)           | -0.0733603 (33.82%)       | 0.541163 (2.31%)           | -0.104423 (5.97%)         |
| $0.2 \times 10^{-6}$  | 0.539698 (2.58%)           | -0.0929913 (5.57%)        | 0.562811 (1.63%)           | -0.103201 (4.87%)         |
| $0.3 \times 10^{-6}$  | 0.555371 (0.31%)           | -0.0972333 (0.96%)        | 0.545887 (1.42%)           | -0.0950575 (3.28%)        |
| $0.4 \times 10^{-6}$  | 0.553427 (0.04%)           | -0.0972030 (0.99%)        | 0.556465 (0.51%)           | -0.100011 (1.84%)         |
| $0.11 \times 10^{-4}$ | 0.558741 (0.91%)           | -0.0972420 (0.96%)        | 0.558570 (0.88%)           | -0.0988116 (0.65%)        |
| $0.38 \times 10^{-3}$ | 0.556832 (0.57%)           | -0.0972831 (0.91%)        | 0.559778 (1.1%)            | -0.0992930 (1.13%)        |
| $0.14 \times 10^{-1}$ | 0.570252 (2.91%)           | -0.0991591 (1.0%)         | 0.565068 (2.02%)           | -0.0997895 (1.62%)        |
| 0.15                  | 0.673473 (17.79%)          | -0.110139 (10.87%)        | 0.517201 (7.05%)           | -0.0935173 (4.65%)        |

for a bimaterial plane with an interface crack are presented in the brackets as well. It can clearly be seen that the obtained results depend on the value  $r_0/L$  and on the adjustment conditions. Particularly, the values of  $K_1$  and  $K_2$  obtained for very small (two first lines of the table) and very large (two last lines) magnitudes of  $r_0/L$  may differ significantly from the exact values. As a rule, the solution obtained by means of the conditions (34) gives more accurate results than the conditions (35). Nevertheless, the results obtained for the range  $r_0/L = 0.3 \times 10^{-6} - 0.38 \times 10^{-3}$  show an excellent agreement with the exact solution, especially for the adjustment conditions (34). Therefore, for practical applications, it is recommended to use the mentioned interval of  $r_0/L$  and the adjustment conditions (34), as it is done for the following calculations.

Table 2 shows the results for the SIFS with various values of  $r_0$  for purely mechanical loading (columns 2, 3) and for combined electromechanical loading ( $\sigma_{33}^{ext} = 10\text{MPa}$ ,  $D_3^{ext} = 0.01\text{C}/\text{m}^2$ , columns 4, 5). From Table 2, one can conclude that the SIFS depend only on the material constants and the applied mechanical loads, and they do not depend on the applied electric loads. This agrees with similar conclusions concerning a crack in a homogeneous material, [8].

Figure 4 shows the distributions at stress components  $\sigma_{33}(r, 0)$  and  $\sigma_{13}(r, 0)$  at the interface and Figure 5 shows the displacement jump  $[u_3(r)]$  and the electrical displacement  $D_3(r, \pi)$  along the crack faces plotted as functions of the distance from the crack tip. These results have been obtained for purely mechanical loading ( $\sigma_{33}^{ext} = 10\text{MPa}$ ) and for  $r_0/L = 0.4 \times 10^{-6}$ . The solution obtained by means of the usual FE computations is compared with solutions following from the technique introduced above and with the exact analytical solution. The results confirm the conclusion of the paper [10] that, in general, the usual FEM cannot give correct results at interface crack tips. On the other hand, there is an excellent agreement between the developed approach and the exact analytical solution.

## 5

### Conclusions

An analytical-numerical approach for analyzing the interface crack between dissimilar piezoelectric materials has been presented. This approach consists of the combination of the asymptotic solution at the crack tip with the conventional FE solution of the corresponding boundary value problem for the interface crack in a piezoelectric bimaterial. The benefit of the method has been demonstrated by conducting several test cases. The results of the test show that, in contrast to the standard displacement-based FEM, the present approach can

**Table 2.** Comparison of exact and numerical values of stress intensity factors for different applied loads

| $r_0/L$              | Purely mechanical loading<br>$\sigma_{33}^{ext} = 10\text{MPa}$ |                           | Combined electromechanical loading<br>$\sigma_{33}^{ext} = 10\text{MPa}$ , $D_3^{ext} = 0.01\text{C}/\text{m}^2$ |                           |
|----------------------|---|---------------------------|--|---------------------------|
|                      | $K_1(\text{MPa}\sqrt{m})$                                       | $K_2(\text{MPa}\sqrt{m})$ | $K_1(\text{MPa}\sqrt{m})$  | $K_2(\text{MPa}\sqrt{m})$ |
| $0.1 \times 10^{-6}$ | 0.512257  | -0.0733603                | 0.512561   | -0.0733844                |
| $0.2 \times 10^{-6}$ | 0.539698  | -0.0929913                | 0.539710   | -0.0930277                |
| $0.3 \times 10^{-6}$ | 0.555371  | -0.0972333                | 0.555390   | -0.0972763                |
| $0.4 \times 10^{-6}$ | 0.553427  | -0.0972030                | 0.553446   | -0.0972429                |



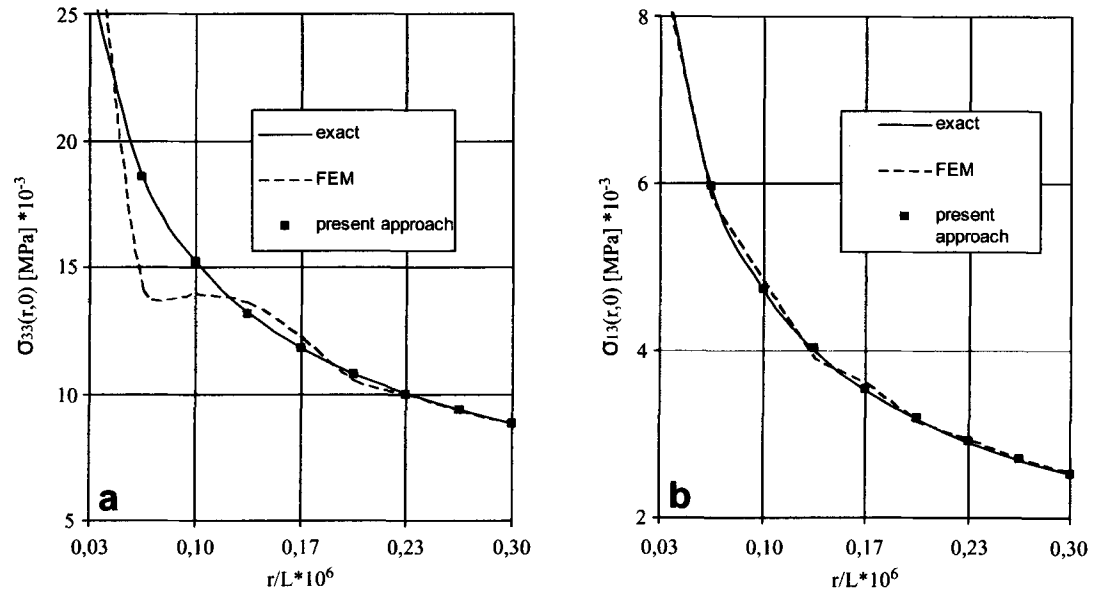


Fig. 4. Distribution of the normal stress (a) and the shear stress (b) along the interface

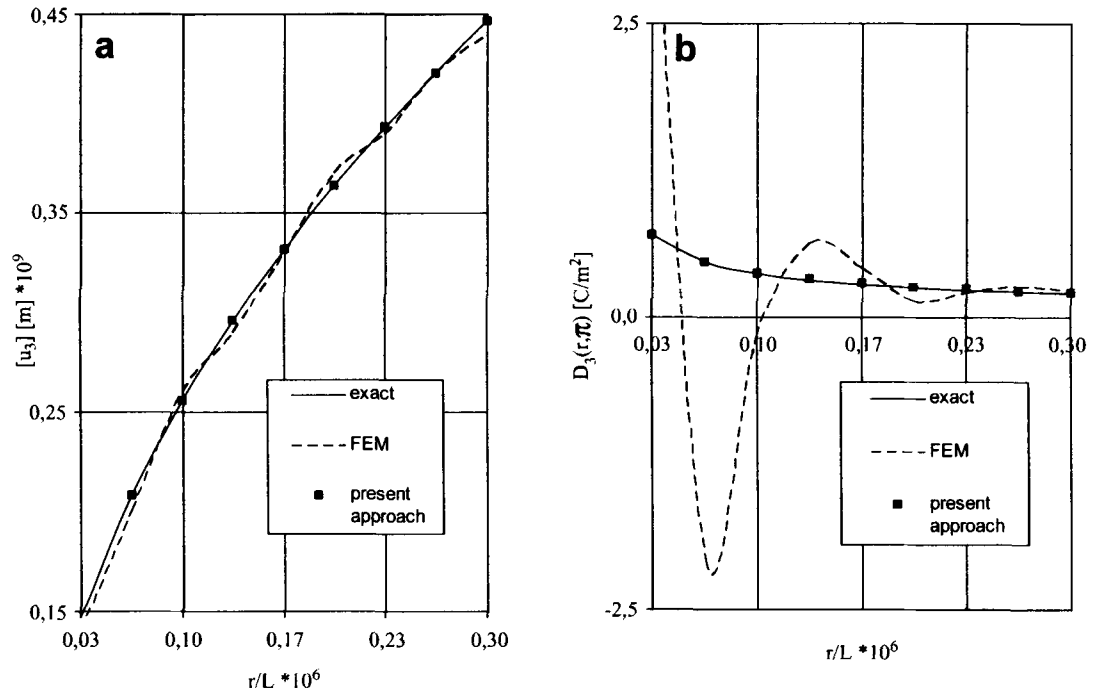


Fig. 5. Distribution of the displacement jump (a) and the electrical displacement (b) along the crack faces

efficiently simulate the singular fields near the crack tip. Furthermore, the SIF can easily and correctly be extracted. Comparison of the field distributions and the SIFs obtained with this approach for a relatively short crack with respect to the domain-size exhibits good correlation with the exact analytical solution obtained for an interface crack in an infinite bimaterial plane. The computed results confirm that under the permeable boundary condition at the crack faces electromechanical fields induced by the crack depend only on the applied mechanical loading. This means that the applied electrical loading has no effect on these fields.

## References

1. Parton, V.Z.: Fracture mechanics of piezoelectric materials. *Acta Astronaut* 3 (1976) 671–683
2. Pak, Y.E.: Linear electro-elastic fracture mechanics of piezoelectric materials. *Int J Fracture* 54 (1992) 79–100
3. Sosa, H.: On the fracture mechanics of piezoelectric solids. *Int J Solids Struct* 29 (1992) 2613–2622
4. Suo, Z.; Kuo, C.M.; Barnett, D.M.; Willis, J.R.: Fracture mechanics for piezoelectric ceramics. *J Mech Phys Solids* 40 (1992) 739–765
5. Govorukha, V.B.; Munz, D.; Kamlah, M.: On the singular integral equations approach to the interface crack problem for piezoelectric materials. *Arch Mech* 52 (2000) 247–273
6. Kuna, M.: Finite element analyses of crack problems in piezoelectric structures. *Compu Mat Sci* 13 (1998) 67–80
7. Wu, C.C.; Sze, K.Y.; Huang, Y.Q.: Numerical solutions on fracture of piezoelectric materials by hybrid element. *Int J Solids Struct* 38 (2001) 4315–4329
8. Gruebner, O.; Kamlah, M.; Munz, D.: Finite element analysis of cracks in piezoelectric materials taking into account the permittivity of the crack medium. *Eng Fracture Mech* 70 (2003) 1399–1413
9. Kemmer, G.: Berechnung von elektromechanischen Intensitätsparametern bei Rissen in Piezokeramiken. PhD-thesis, Technische Universität Dresden. VDI-Verlag; Düsseldorf: (2000)
10. Scherzer, M.; Kuna, M.: Asymptotic analysis of interface problems in piezoelectric composite materials. In: Hoffmann, K.H., ed., *Smart Materials* Springer, Berlin Heidelberg New York (2001) pp. 137–148
11. Parton, V.Z.; Kudryavtsev, B.A.: *Electromagnetoelasticity*. Gordon and Breach; New York (1998)
12. Kuo, C.M.; Barnett, D.M.: Stress singularities of interfacial cracks in bounded piezoelectric half-spaces. In: (Wu, J.J., Ting, T.C.T., Barnett, D.M. eds.) *Modern theory of anisotropic elasticity and applications* SIAM Proc Series, Philadelphia, (1991) pp. 33–50
13. Ting, T.C.T.: Explicit solution and invariance of the singularities at an interface crack in anisotropic composites. *Int J Solids Struct* 22 (1986) 965–983
14. ABAQUS/Standard: Version 6.1. Karlsson & Sorensen Inc., Hibbith (2000)
15. Park, S.B.; Sun, C.T.: Effect of electric field on fracture of piezoelectric ceramics. *Int J Fracture* 70 (1995) 203–216
16. Herrmann, K.P.; Loboda, V.V.: Fracture-mechanical assessment of electrically permeable interface cracks in piezoelectric bimetals by consideration of various contact zone models. *Arch Appl Mech* 70 (2000) 127–143
17. Rice, J.R.: Elastic fracture mechanics concepts for interfacial cracks. *J Appl Mech* 55 (1988) 98–103